Available online at www.sciencedirect.com
SCIENCE DIRECT
Carbohydrate Polymers 63 (2006) 198–204
Carbohydrate Polymers
www.elsevier.com/locate/carbpol

Morphological, thermal and mechanical properties of ramie crystallites—reinforced plasticized starch biocomposites

Yongshang Lu [a,*], Lihui Weng [b], Xiaodong Cao [c]

[a] Department of Chemistry, Iowa State University, Ames, IA 50011, USA
[b] Department of Biomedical Engineering, State University of New York at Stony Brook, NY 11794-2580, USA
[c] Department of Chemistry, Wuhan University, Wuhan 430072, People's Republic of China

Received 15 June 2005; revised 7 August 2005; accepted 18 August 2005
Available online 6 October 2005

Abstract

A series of environmentally friendly glycerol plasticized starch (PS) biocomposites were successfully prepared, using ramie cellulose nanocrystalites (RN) of 0–40 wt% as fillers. The ramie cellulose nanocrystalites, having lengths of 538.5 ± 125.3 nm and diameters of 85.4 ± 25.3 nm on average, were prepared from ramie fibers by acid hydrolysis. The morphology, thermal behavior and mechanical properties of the resulting composites were investigated by scanning electron microscopy, differential scanning thermal analysis, dynamic mechanical thermal analysis, and measurements of mechanical properties and water absorption. The results indicate that the synergistic interactions between fillers and between filler and PS matrix play a key role in reinforcing the composites. The PS/RN composites, conditioned at 50% relative humidity, increases, respectively, in both tensile strength and Young's modulus from 2.8 MPa for PS film to 6.9 MPa and from 56 MPa for PS film to 480 MPa with increasing RN content from 0 to 40 wt%. Further, incorporating RN fillers into PS matrix also leads to a decrease in water sensitivity for the PS based biocomposites.

Keywords: Starch; Cellulose nanocrystalites; Biocomposite; Ramie

1. Introduction

Advanced technology in the field of petrochemical-based polymers has brought many benefits to mankind. However, it is becoming more evident that the ecosystem is considerably disturbed and damaged as a result of the non-degradable plastic materials for disposable items. So there is an urgent need to develop renewable source-based environmental benign materials, which are novel materials of the 21st century and would be of great importance to the materials world, not only as a solution to growing environmental threat but also as a solution to the uncertainty of petroleum supply (Fishman, Coffin, Onwulata & Konstance, 2004; Lu, Tighzert, Berzin & Rondot, 2005; Lu, Weng, & Zhang, 2004; Mohanty, Misra, & Drzal, 2002; Ray & Okamoto, 2003). Among the many kinds of candidates of biodegradable polymers, starch is one of the most promising materials for biodegradable plastics because it is a versatile biopolymer with immense potential and low price for use in the non-food industries (Choi, Kim, & Park, 1999; Mohanty, Misra, & Hinrichsen, 2000). Incorporating plastifying agent, such as water and /or poly-alcohols, starch can be made thermoplastic called thermoplastic starch (TPS) or plasticized starch (PS) through destructurization by the introduction of mechanical and heat energy (Carvalho, Job, Alves, Curvelo, & Gandini, 2003; Gaudin, Lourdin, Forssell, & Colonna, 2000). During the past two decades, PS has received considerable attention and offered an interesting alternative for synthetic polymers where long-term durability is not needed and rapid degradation is an advantage (Van Soest, De Wit, & Vliegenthart, 1996). However, compared to the common thermoplastics, biodegradable products based on starch, unfortunately, still reveal many disadvantages, mainly attributed to the highly hydrophilic character of starch polymers (Santayanon & Wootthikanokkhan, 2003). To cope with these problems while persevering the biodegradability of the materials, one of the effective strategies is to associate PS with various fillers derived from renewable resources to obtain the biocomposites. Various types of fillers have been tested such as potato pulp based microfibrils (Dufresne, Dupeyre, & Vignon, 2000; Dufresne & Vignon, 1998), bleached leafwood fibres (Averous & Boquillon, 2004; Funke, Bergthaller, &

* Corresponding author. Tel.: +1 515 2949803
E-mail address: ysluchem@yahoo.com (Y. Lu).

0144-8617/$ - see front matter © 2005 Elsevier Ltd. All rights reserved.
doi:10.1016/j.carbpol.2005.08.027

Lindhauer, 1998), bleached eucalyptus pulp fibres (Curvelo, De Carvalho, & Agnelli, 2001), wood pulp (De Carvalho, Curvelo, & Agnelli, 2002), flax and jute fibers (Soykeabkaew, Supaphol, & Rujiravanit, 2004; Wollerdorfer & Bader, 1998) and tunicin whiskers (Anglès & Dufresne, 2000; Anglès & Dufresne, 2001; Mathew, & Dufresne, 2002). The researches mentioned above indicated that a high compatibility occurs between starch matrix and fillers and the high improvements of the performances (e.g. mechanical properties and water resistance) due to the occurrence of intermolecular interactions formed between the different components.

It is known that native celluloses, when subjected to strong acid hydrolysis, readily break down into 'micro- or nano-crystalline cellulose' (whisker) with almost no weight loss (Battista, 1975; Ebeling et al., 1999). Due to its high aspect ratio and a high Young's modulus (Ishikawa, Okano, & Sugiyama, 1997), the use of cellulose crystallites for preparation of high performance composite materials has been, therefore, explored extensively (Dufresne, Cavaillé, & Vignon, 1997; Eichhorn et al., 2001; Noishiki, Nishiyama, Wada, Kuga, & Magoshi, 2002; Anglès et al., 2000, 2001). When the cellulose crystallites were homogeneously dispersed into polymer matrices, they gave a remarkable reinforcing effect, even at concentrations of a few percent (Favier, Chanzy, & Cavaille, 1996).

Ramie, or China grass (*Boehmeria nivea* (L.) Gaud.) is a perennial herbaceous plant of the Urticaceous family. This crop is mainly planted in China and other Asian countries including Philippines and India. Ramie fibers have been used as a textile fiber for centuries due to their excellent fiber chacteristics (Angelini, Lazzeri, Levita, Fontanelli, & Bozzi, 2000). Ramie fibers are very fine and silk-like, naturally white in color, and have a high luster. Other advantages of it are good resistance to bacteria, mildew, and insect attack. The fibers are stable in alkaline media and not harmed by mild acids. Further, it also exhibits even greater strength when wet (Mohanty, Misra, & Drzal, 2005). Due to the excellent fiber properties mentioned above, ramie fibers have, therefore, a high potential as a reinforcing fiber for polymer composites. In this work, we want to prepare cellulose nanocrystallites from ramie fiber by acid hydrolysis, and then use the resulting nanocrystallites to reinforce the plasticized starch for preparation of high performance biocomposites. The resulting materials were prepared by casting the aqueous dispersion of cellulose nanocrystalites and glycerol plasticized starch in various blend ratios. The morphology, structure and performance improvement of the biocomposites were investigated by scanning electronic microscopy, dynamic mechanical thermal analysis, differential scanning calorimetry, and measurements of the mechanical properties and water absorption.

2. Materials and methods

2.1. Materials

Purified ramie fiber was supplied by Textile Factory, Xianning. The starch used in this work is commercial industrial-grade wheat starch, which is composed of 25% amylose and 75% amylopectin. The glycerol (99.5% purity) was purchased from Aldrich and used as received.

2.2. Preparation of ramie cellulose nanocrystallites

The suspensions were prepared by acid catalyzed hydrolysis of ramie fiber similar to the method as described by Dong, Kimura, Revol, and Gray (1996). Briefly, the ramie fiber (20 g) was mixed with sulfuric acid (175 mL, 64%) and stirred vigorously at 45 °C for 4 h, and then a dispersion of ramie cellulose nanocrystalites (RN) was obtained. After sonication of 15 min, the suspension was neutralized with 0.5 N NaOH and then washed by dialysis. The final aqueous suspension of RN does not sediment or flocculate because of the electrostatic repulsion between the surface sulfate groups grafted during the sulfuric acid treatment (Chazeau, Paillet, & Cavaillé, 1999).

2.3. Preparation of plasticized starch (PS)/RN biocomposites

Starch and glycerol were first mixed and dispersed in distilled water. The mixture contained 7 wt% wheat starch, 3 wt% glycerol and 90 wt% water, respectively. The gelatinization of starch was performed in a sealed reactor equipped with a stirrer operating at 100 °C for 20 min. The resulting starch pastes were cooled down to 70 °C in order to prevent evaporation of water. Subsequently, the RN dispersion was added and stirred for 20 min. After mixing, the mixture was degassed under vacuum and cast in a polystyrene mold, followed by drying in an oven at 40 °C and 50% relatively humidity. By changing the content of RN of 0, 5, 10, 15, 20, 25, 30, 40 wt%, a series of PS/RN biocomposites were prepared and coded as PS, SR-5, SR-10, SR-15, SR-20, SR-25, SR-30 and SR-40, respectively, in which the RN content was expressed on water free PS matrix.

Before various characterizations, the resulting composite films, with a thickness of about 0.3 mm, were kept in a conditioning cabinet of 50% relative humidity (RH) at 25 °C, respectively, to ensure the equilibration of the water content in the films.

2.4. Characterizations

Atomic force microscopy (AFM) imaging of RN was performed on a Digital 3100 IIIa microscope. A droplet of a dilute RN suspension was coated onto a flake of mica, and the water was evaporated at room temperature.

The DSC analysis of the biocomposites was determined using a modulated differential scanning calorimeter (TA2920, USA) with refrigerator cooler. Each sample conditioned at 50% RH was subjected to the heating/cooling cycle between −50 °C and 100 °C to obtain reproducible glass temperature (T_g) values. For a polymer, T_g was taken at the half-variation of the heat capacity in the second run occurring at the glass–rubber transition. Scanning rate in the second run was 5 °C/min.

Dynamic mechanical behavior of the biocomposites were determined with a dynamic mechanical thermal analyzer (DMTA-V, Rheometric Scientific Co., USA) at 1 Hz and a heating rate of 5 °C/min in the temperature range from −90 to 150 °C. The specimens with typical size of 10 mm × 5 mm (length × width) were used.

Morphology of the biocomposites was observed with a scanning electron microscope (S-570, Hitachi, Japan) at 20 kV. The specimens were frozen in liquid nitrogen, fractured, and then coated with gold.

The tensile strength, elongation at break and Young's Modulus of the composites were determined with a mechanical testing machine (Test 110 from GT Test, France), with a crosshead speed of 10 mm/min. The dumb-bell specimens of 17 mm × 4 mm (length × width) were used. An average value of at least eight replicates of each specimen was taken.

The dried films of 20 mm × 20 mm with a thickness of about 0.3 mm, immersed at 0% RH (P_2O_5) atmosphere for one week, were weighed and conditioned at 25 °C in a chamber containing $CuSO_4 \cdot 5H_2O$ saturated solution to ensure a of 98% RH. The samples were removed at desired intervals and weighed until the equilibrium state was reached. The water uptake (WU) of the samples was calculated as follows:

$$\mathrm{WU}(\%) = \frac{M_t - M_0}{M_0} \times 100 \quad (1)$$

where M_t and M_0 are the weight of the sample at time t in 98% RH and the initial weight of the sample before exposure to 98% RH, respectively.

3. Results and discussion

3.1. Morphology of RN and the PS/RN biocomposites

The AFM image of a dilute suspension of ramie nanocrystallies is shown in Fig. 1. The suspension consists of individual RN fragments having a spindle shape. These fragments have a broad distribution in length (L) ranging from 350 to 700 nm but relatively uniform diameter (D) ranging from 70 to 120 nm. The average of length and diameter were estimated to be 538.5 ± 125.3 nm and 85.4 ± 25.3 nm, respectively. Therefore, the average aspect ratio, L/D, is nearly 6, which is slight lower compared with about 10 for cotton based cellulose crystallites (Ebeling et al., 1999; Lu, Weng, & Cao, submitted for publication).

The SEM images of RN filled PS biocomposites are shown in Fig. 2. It is very easy to identify the occurrence of the RN fillers in the PS matrix, but difficult to identify the individual filler dispersion due to its small size. However, some fillers appeared as white domain at the fractured surface of samples. That should correspond to the filler in the perpendicular plane of the composites. No large agglomerates of the fillers and good adhesion between the matrix and fillers are observed, which should play an important role in improving the mechanical performance and water resistance of the resulting materials as discussed later.

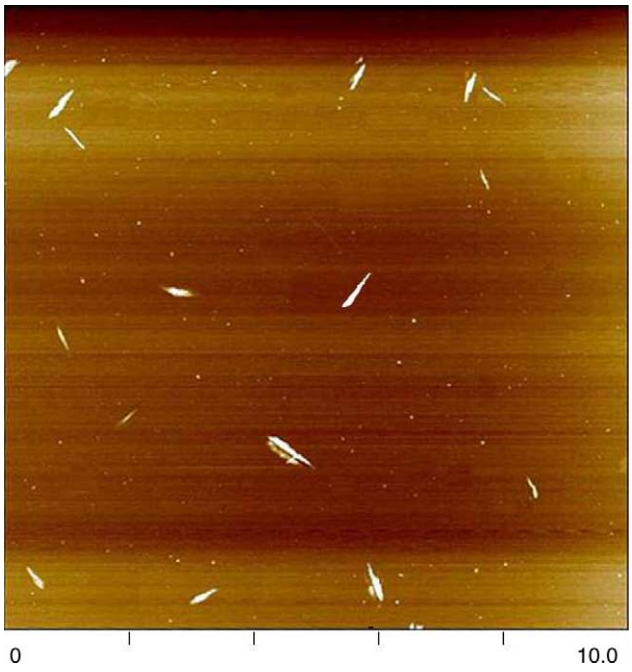

Fig. 1. The AFM imaging of ramie nanocrystallites from a dilute suspension (scale bar = 2 μm).

3.2. Thermal analysis

Figure 3 shows the DSC curves in the temperature region of −40 to 100 °C of the PS/RN composites conditioned at 50% relative humidity. No endothermic peaks, assigned to the melting of water-induced crystalline amylopectin domains (Mathew & Dufresne, 2002), is observed in the temperature region of 100–200 °C (not shown), indicating the amorphous nature of the plasticized starch matrix. The PS film exhibits a T_g transition at about 26.8 °C. The PS formulation used here is in the case of a complex heterogeneous system composed of glycerol-rich domains dispersed in an starch rich continuous phase (Averous & Boquillon, 2004), and each phase should exhibit its own T_g transition. Therefore, the transition at 26.8 °C can be associated with glass transitions of starch-rich phase. The T_g transition of glycerol rich phase located in the temperature region from −80 to −50 °C, unfortunately, cannot be determined because of the limitation of refrigerated cooling systems of DSC. By incorporating RN fillers of 0–40 wt% into PS matrix, the T_g transition for starch rich phase shifts to higher temperature from 26.8 to 55.7 °C. The increase in T_g dependence of the content of RN fillers might be attributed to the occurrence of intermolecular interactions occurred between starch and stiff crystallites, which reduces the flexibility of molecular chains of starch.

Figure 4 shows the temperature dependence of dynamic mechanical thermal analysis behaviors for the PS/RN biocomposites. The maximum of tan δ peak, which corresponds to the glass transition temperature, is often different from the T_g determined with DSC. Such a difference is very common due to the nature difference between two measure techniques. DSC measures the change in heat capacity going from the frozen to the unfrozen chain, whereas DMA measures

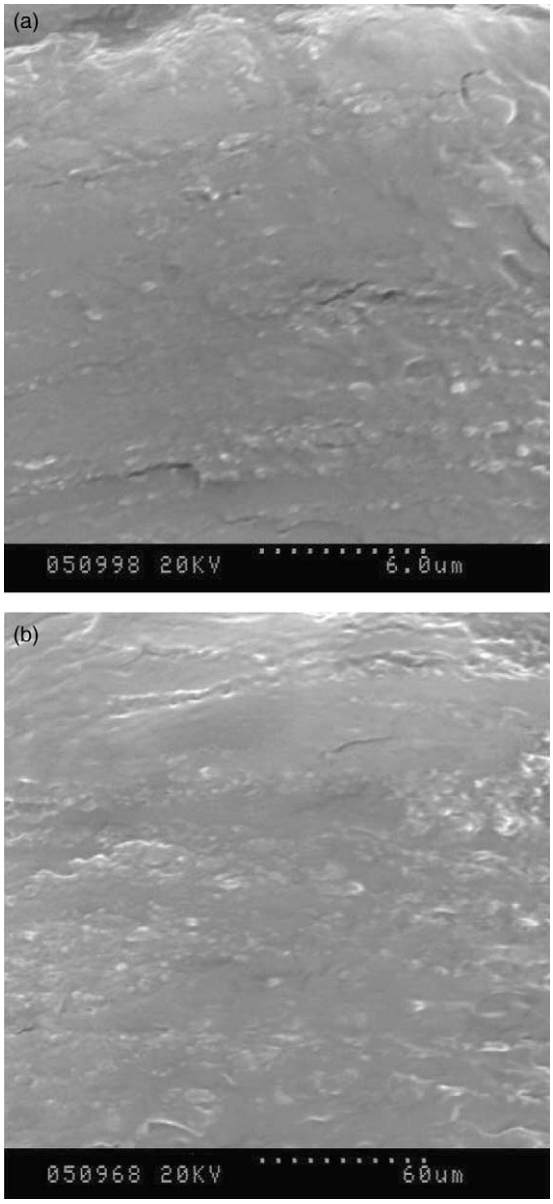

Fig. 2. The SEM imaging of (a) SR-15 and (b) SR-30.

the change in mechanical response of these chains. Two techniques give the effectively different averages of the complex dynamics of chain motion (Rouilly, Rigal, & Gilbert, 2004; Wunderlich, 1990). In Fig. 4a, a two-step decrease of the storage modulus in the temperature region from −75 to −40 °C and from 0 to 50 °C, attributed, respectively, to the T_g transitions of glycerol rich phase and starch rich phase, is observed for PS and all PS based composites. However, compared with PS film, the composites exhibit an increase in storage modulus over entire studied temperature region. For example, the storage modulus of the composite filled with 30 wt% RN fillers is, respectively, about 15 and 10 times higher than that of PS film at 25 and 100 °C, indicating a higher thermal stability of the resulting composites. This can be attributed to the strong interfacial interactions through hydrogen bonding between large specific surface of RN and

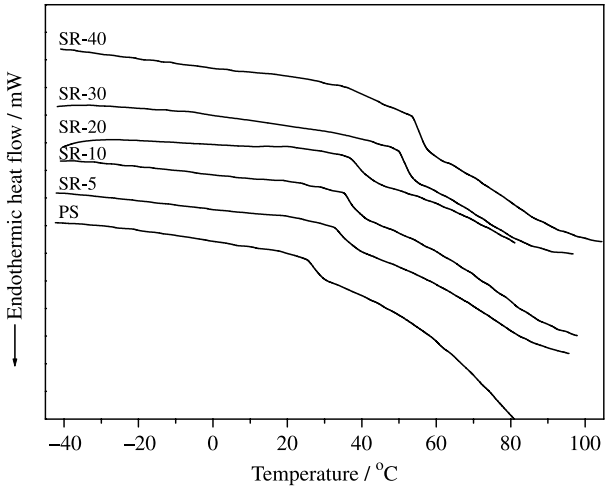

Fig. 3. DSC curves of PS film and PS/RN biocomposites.

starch matrix (Anglès & Dufresne, 2000; Anglès & Dufresne, 2001).

The tan δ–T curves (Fig. 4b) of PS and all composites show two relaxation processes at lower and higher temperature, corresponding, respectively, to the T_gs of the glycerol rich phase and starch rich phase. With increasing the fillers content from 0 to 30 wt%, no shifting of position and width change of

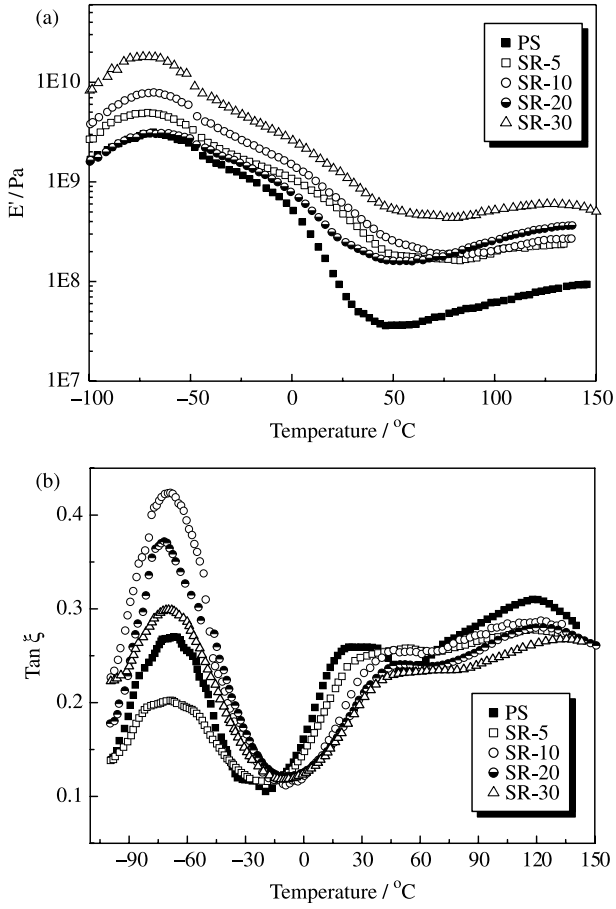

Fig. 4. The dynamic mechanical behaviors of both storage modulus (E') and loss factor (tan δ) as a function of temperature for PS film and PS/RN biocomposites.

tan δ peak at lower temperature are found. However, the loss peak of starch rich phase at higher temperature shifts from 26 to 46.5 °C accompanied by flat peak, indicating that RN fillers restrict molecular motions of starch, due to the strong interaction between starch and fillers (Park et al., 2002). This is in good agreement with the results from DSC.

3.3. Mechanical properties

The mechanical properties of the PS/RN biomposites, such as Young's modulus, tensile strength and elongation at break, are shown in Fig. 5, and their corresponding stress–strain curves are presented in Fig. 6. The tensile strength and Young's modulus of the films increase significantly from 2.8 to 6.9 MPa and from about 55.9 to 479.8 MPa with increasing fillers content from 0 to 40 wt%, whereas the elongation at break decreases from 94.2% to 13.6%. The mechanical behaviors of the composites in this work are different from that of tunicin cellulose whisker reinforced waxy maize starch composites (Anglès & Dufresne, 2001), in which a relatively very low reinforcing effect is reported upon the addition of tunicin whiskers due to the competitive interactions between the components and a plasticizer accumulation in the cellulose/amylopectin interfacial zone. This plasticizer accumulation phenomenon most probably interferes with hydrogen-bonding forces that are likely to hold the percolating cellulose whiskers network within the matrix. Fig. 6 shows stress–starin curves of PS and the PS based composites at room temperature. Generally, the films exhibit two characteristic regions of deformation behavior in their tensile stress–strain curves. At low strains (<10%) the stress increases rapidly with an increase in strain. The initial slopes were steep in the elastic region, indicating the relative high elastic moduli of these materials. At higher strain (> 10%) the films show a slow increase in stress with increasing strain until failure occurs with no necking. It is indicative of the relatively homogeneous nature of these biocomposites as seen in SEM.

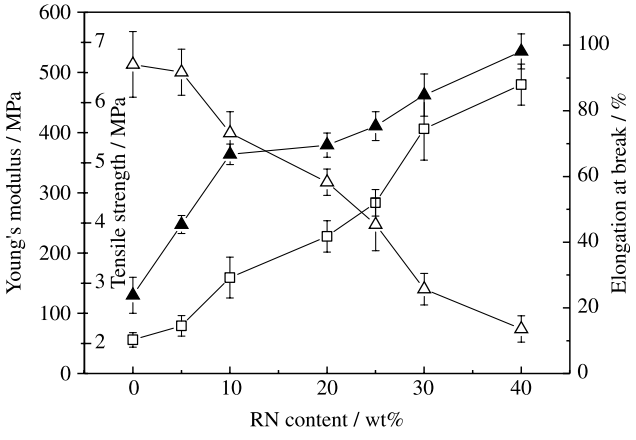

Fig. 5. The mechanical behaviors of Young's modulus (□), tensile strength (▲) and elongation at break (△) of PS films as a function of RN content.

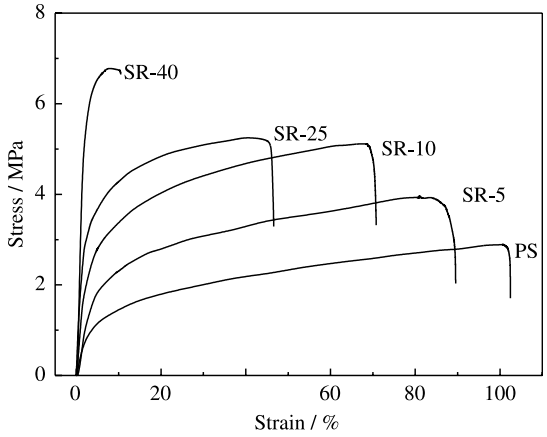

Fig. 6. The stress–strain curves for PS film and PS/RN biocomposites.

3.4. Surface properties and water absorption

Figure 7 shows the water uptake of PS and RN filled composites during conditioning in 98% RH as a function of time. The water uptake—t curves display two well-separated zones. At shorter times, $t<100$ h, the kinetics of absorption is very fast, whereas at longer times, $t>100$ h, the kinetics of absorption is slow and leads to a plateau, corresponding to the water uptake at equilibrium. The water uptake at equilibrium of PS films as a function of RN content is plotted in Fig. 8. The starch film absorbs about 63 wt% water. It is indicative of about 1.63 g of water absorbed per gram of starch. The water uptake at equilibrium decreases non-lineally with increasing the content of RN fillers, and about 45 wt% of water uptake is observed for the composites containing 40 wt% fillers. Compared with PS, The composites display a reduced swelling capacity. The kinetic study of the sorption in polymers as a means of determining the diffusion coefficient has widely been used. In general, the partial differential equation for mass transfer (diffusion) is expressed as (Vergnaud, 1991)

$$\frac{\partial C}{\partial t} = D\left(\frac{\partial^2 C}{\partial x^2}\right)$$

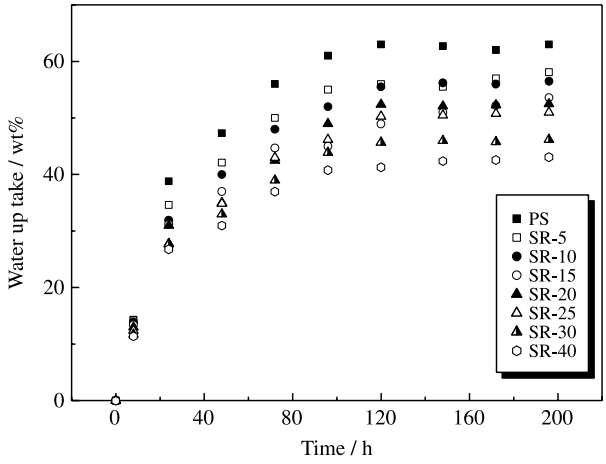

Fig. 7. Water uptake of the PS film and PS/RN bicomposites during conditioned at 98% RH as a function of time.

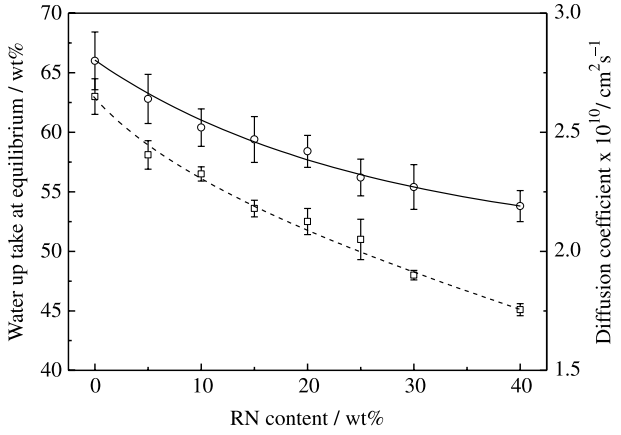

Fig. 8. Water uptake at equilibrium (□) and diffusion coefficient (○) of the PS film conditioned at 98% RH as a function of RN content. Results are the average values of quadruplicate.

where C is the concentration at time t, and distance x, from the polymer surface. For an infinite slab with a constant D and at short times:

$$\frac{M_t - M_0}{M_\infty} = \frac{4}{L}\left[\frac{Dt}{\pi}\right]^{1/2}$$

M_t and M_0 are the weight of the sample at time t in 98% RH and the initial weight of the sample before exposure to 98% RH, respectively. M_∞ is the equilibrium water sorption, and L is the thickness of the sample. The ratio of the amount of water absorbed by the specimen at time t, $(M_t - M_0)/M_\infty$, was plotted as a function of $t^{1/2}$, and the diffusion coefficient (D) was, therefore, calculated from the slope of the initial linear part of the resulting curves. As shown in Fig. 8, the PS film shows the highest D value of about 2.80×10^{-10} cm^2 s^{-1}. Interestingly, with an increase of fillers in the PS matrix from 0 to 40 wt%, the D value of the composites decreases from 2.80×10^{-10} to 2.19×10^{-10} cm^2 s^{-1}. This phenomenon can be ascribed to the presence of strong hydrogen bonding interactions between starch matrix and RN. The hydrogen bonding interactions in the composites tend to stabilize the starch matrix when submitted to very moist atmosphere. Meanwhile, both high crystallite of cellulose and relative low glycerol content in the PS/RN composite also might be responsible for the reduction of water uptake at equilibrium and water diffusion coefficient of the resulting materials (Funke, Bergthaller, & Lindhauer, 1998).

4. Conclusions

A suspension of cellulose nanocrystallites (RN), with an average length of about 538.5 ± 125.3 nm and diameters of 85.4 ± 25.3 nm, was prepared from ramie fibers by acid hydrolysis and used to reinforce the PS matrix for preparation of biocomposites by casting method. The SEM shows a relatively good dispersion of the RN fillers in the PS matrix and good adhesion between the matrix and fillers. It is worth noting that the RN filled PS composites show an increase in Young's modulus and tensile strength from 56 to 480 MPa and 2.8 to 6.9 MPa with increasing fillers content from 0 to 40 wt%. As the RN fillers increase in the PS matrix, the resulting composites show a higher water-resistance. The performance improvement of these PS/RN biocomposites may be ascribed to three-dimensional networks of intermolecular hydrogen bonding interactions between filler and filler and between fillers and PS matrix.

References

Angelini, L. G., Lazzeri, A., Levita, G., Fontanelli, D., & Bozzi, C. (2000). Ramie (*Boehmeria nivea* (L.) Gaud.) and Spanish Broom (*Spartium junceum* L.) fibres for composite materials: agronomical aspects, morphology and mechanical properties. *Industrial Crops and Products*, *11*, 145–161.

Anglès, M. N., & Dufresne, A. (2000). Plasticized/tunicin whiskers nanocomposites. 1. Structural analysis. *Macromolecules*, *33*, 8344–8353.

Anglès, M. N., & Dufresne, A. (2001). Plasticized/tunicin whiskers nanocomposites materials. 2. Mechanical behaviour. *Macromolecules*, *34*, 2921–2931.

Averous, L., & Boquillon, N. (2004). Biocomposites based on plasticized starch: thermal and mechanical behaviours. *Carbohydrate Polymers*, *56*, 111–122.

Battista, O. A. (1975). *Microcrystal polymer science*. New York: McGraw-Hill Book Company.

Carvalho, A. J. F., Job, A. E., Alves, N., Curvelo, A. A. S., & Gandini, A. (2003). Thermoplastic starch/natural rubber blends. *Carbohydrate Polymer*, *53*, 95–99.

Chazeau, L., Paillet, M., & Cavaillé, J. Y. (1999). Plasticized PVC reinforced with cellulose whiskers. I. Linear viscoelastic behavior analyzed through the quasi-point defect theory. *Journal of Polymer Science Part B: Polymer Physics*, *37*, 2151–2164.

Choi, E. J., Kim, C. H., & Park, J. K. (1999). Structure–property relationship in PCL/starch blend compatibilized with starch-*g*-PCL copolymer. *Journal of Polymer Science Part B: Polymer Physics*, *37*, 2430–2438.

Curvelo, A. A. S., De Carvalho, A. J. F., & Agnelli, J. A. M. (2001). Thermoplastic starch–cellulosic fibers composites: Preliminary results. *Carbohydrate Polymers*, *45*, 183–188.

De Carvalho, A. J. F., Curvelo, A. A. S., & Agnelli, J. A. M. (2002). Wood pulp reinforced thermoplastic starch composites. *International Journal of Polymer Materials*, *51*, 647–660.

Dong, X. M., Kimura, T., Revol, J-F. , & Gray, D. G. (1996). Effects of ionic strength on the isotropic-chiral nematic phase transition of suspensions of cellulose crystallites. *Langmuir*, *12*, 2076–2082.

Dufresne, A., Cavaillé, J-Y. , & Vignon, M. R. (1997). Mechanical behavior of sheets prepared from sugar beet cellulose microfibrils. *Journal of Applied Polymer Science*, *64*, 1185–1194.

Dufresne, A., Dupeyre, D., & Vignon, M. R. (2000). Cellulose microfibrils from potato tuber cells: Processing and characterization of starch–cellulose microfibril composites. *Journal of Applied Polymer Science*, *76*, 2080–2092.

Dufresne, A., & Vignon, M. R. (1998). Improvement of starch film performances using cellulose microfibrils. *Macromolecules*, *31*, 2693–2696.

Ebeling, T., Paillet, M., Borsali, R., Diat, O., Dufresne, A., Cavaille, J-Y. , et al. (1999). Shear-induced orientation phenomena in suspensions of cellulose microcrystals, revealed by small angle X-ray scattering. *Langmuir*, *15*, 6123–6126.

Eichhorn, S. J., Baillie, C. A., Zafeiropoulos, N., Mwaikambo, L. Y., Ansell, M. P., Dufresne, A., et al. (2001). Current international research into cellulosic fibres and composites. *Journal of Materials Science*, *36*, 2107–2131.

Favier, V., Chanzy, H., & Cavaille, J. Y. (1996). Polymer nanocomposites reinforced by cellulose whiskers. *Macromolecules*, *28*, 6365–6367.

Fishman, M. L., Coffin, D. R., Onwulata, C. I., & Konstance, R. P. (2004). Extrusion of pectin and glycerol with various combinations of orange albedo and starch. *Carbohydrate Polymers*, *57*, 401–413.

Funke, U., Bergthaller, W., & Lindhauer, M. G. (1998). Processing and characterization of biodegradable products based on starch. *Polymer Degradation and Stability*, *59*, 293–296.

Gaudin, S., Lourdin, D., Forssell, P. M., & Colonna, P. (2000). Antiplasticisation and oxygen permeability of starch–sorbitol films. *Carbohydrate Polymers*, *43*, 33–37.

Ishikawa, A., Okano, T., & Sugiyama, J. (1997). Fine structure and tensile properties of ramie fibres in the crystalline form of cellulose I, II, III_I and IV_I. *Polymer*, *38*, 463–468.

Lu, Y., Tighzert, L., Berzin, F., & Rondot, S. (2005). Innovative plasticized starch films modified with waterborne polyurethane from renewable resources. *Carbohydrate Polymers*, *61*, 174–182.

Lu, Y., Weng, L., & Cao, X. (2005). Biocomposites from plasticized starch and cellulose crystallites from cottonseed Linter. *Macromolecular Bioscience*.

Lu, Y., Weng, L., & Zhang, L. (2004). Morphology and properties of soy protein isolate thermoplastics reinforced with chitin whiskers. *Biomacromolecules*, *5*, 1046–1051.

Mathew, A. P., & Dufresne, A. (2002). Morphological investigations of nanocomposites from sorbitol elasticised starch and tunicin whiskers. *Biomacromolecules*, *3*, 609–617.

Mohanty, A. K., Misra, M., & Drzal, L. T. (2002). Sustainable bio-composites from renewable resources: opportunities and challenges in the green materials world. *Journal of Polymer and Environment*, *10*, 19–26.

Mohanty, A. K., Misra, M., & Drzal, L. T. (2005). *Natural fiber, biopolymers, and biocompsoites*. Boca Raton, FL: CRC Press p. 77.

Mohanty, A. K., Misra, M., & Hinrichsen, G. (2000). Biofibres, biodegradable polymers and biocomposites: an overview. *Macromolecular Materials and Engineering*, *276/277*, 1–26.

Noishiki, Y., Nishiyama, Y., Wada, M., Kuga, S., & Magoshi, J. (2002). Mechanical properties of silk fibroin–microcrystalline cellulose composite films. *Journal of Applied Polymer Science*, *86*, 3425–3429.

Park, H. M., Li, X., Jin, C. Z., Park, C. Y., Cho, W. J., & Ha, C. S. (2002). Preparation and properties of biodegradable thermoplastic starch/clay hybrids. *Macromolecular Materials and Engineering*, *287*, 553–558.

Ray, S. S., & Okamoto, M. (2003). Biodegradable polylactide and its nanocomposites: opening a new dimension for plastics and composites. *Macromolecular Rapid Communication*, *24*, 815–840.

Rouilly, A., Rigalb, L., & Gilberta, R. G. (2004). Synthesis and properties of composites of starch and chemically modified natural rubber. *Polymer*, *45*, 7813–7820.

Santayanon, R., & Wootthikanokkhan, J. (2003). Modification of cassava starch by using propionic anhydride and properties of the starch-blended polyester polyurethane. *Carbohydrate Polymers*, *51*, 17–24.

Soykeabkaew, N., Supaphol, P., & Rujiravanit, R. (2004). Preparation and characterization of jute- and flax-reinforced starch-based composite foams. *Carbohydrate Polymers*, *58*, 53–63.

Van Soest, J. J. C., De Wit, D., & Vliegenthart, J. F. C. (1996). Mechanical properties of thermoplastic waxy maize starch. *Journal of Applied Polymer Science*, *61*, 1927–1937.

Vergnaud, J. M. (1991). *Liquid transport process in polymeric materials: Modeling and industrial applications*. Englewood Cliffs, NJ: Prentice Hall.

Wollerdorfer, M., & Bader, H. (1998). Influence of natural fibres on the mechanical properties of biodegradable polymers. *Industrial Crops and Products*, *8*, 105–112.

Wunderlich, B. (1990). *Thermal Analysis*. San Diego: Academic Press.